Journal of Scientific and Technical Research
14 (2) 2024, 67-74
http://www.publishingindia.com/jstr

Recent Advances in Polymer Based Atomic Oxygen Resistance Materials for Space Applications

Narender Singh[1] and Sonia Khanna[2*]
[1]Research Scholar, Advanced Polymeric Materials Research Laboratory, Department of Chemistry and Biochemistry, Sharda University, Greater Noida, Uttar Pradesh, India
[2]Associate Professor, Advanced Polymeric Materials Research Laboratory, Department of Chemistry and Biochemistry, Sharda University, Greater Noida, Uttar Pradesh, India
*Corresponding Author: sonia.khanna@sharda.ac.in

Abstract: In low Earth orbit (LEO), atomic oxygen (AO) presents a significant threat to spacecraft materials due to its highly reactive nature, especially with polymers and other organic compounds. AO exposure can cause surface erosion, mass loss, and reduced structural integrity, ultimately impacting spacecraft performance and longevity. This study examines recent developments in AO-resistant materials, focusing on different types of polymers and specially engineered polymer composites. Atomic oxygen-resistant coatings based on various polymeric systems that include fluorinated polymers, silicones, poly (carborane-siloxane)s, and decarborane-based polymers are discussed. Fluorine-containing polymers also show considerable promise due to their inherent chemical stability against AO. The study further explores innovative nanostructured and hybrid materials that offer a balance of mechanical strength and AO resistance and characterization techniques for the atomic oxygen resistance materials. By identifying and optimizing materials that withstand AO exposure, this research also explains about the methods of sensing of atomic oxygen based on satellite, ultimately contributing to more efficient and cost-effective space missions.

Keywords: Atomic oxygen, Characterization techniques, Low Earth orbit, Polyimide film, Siloxanes.

I. INTRODUCTION

Many innovations and developments have been already achieved in various fields of science and technology but in the field of space exploration, it is very difficult to implement the research in the space environment as compared to the experiments in ground-based laboratories because it is extremely difficult to simulate the space environment. In the present scenario, the space research has been focusing on commercializing the space for our benefits. Efforts are on hypersonic spacecraft that can be useful to explore the space environment. For all this, it is necessary to understand the space environment, particularly, the Low Earth Orbit (LEO) where space stations and surveillance satellites are placed. In LEO environment the following effects on materials used for space station and spacecraft are to be studied: i) atomic oxygen (AO) on the spacecraft materials, ii) debris and micrometeoroids impact, iii) ultra-violet radiation and iv) ultra high vacuum. Generally, in upper atmosphere the diatomic oxygen undergoes photodissociation to form atomic oxygen [1].

$$O_2 + h\nu \rightarrow O^{\cdot} + O^{\cdot} (99\%)$$

$$O^+ + O^- \quad (\leq 1\%)$$

In the LEO environment, AO has higher chance of survival due to ultra high vacuum due to which the particle density is very low [2]. Hence, AO can attack materials of space station and spacecraft. Materials that are susceptible to degradation in LEO are to be protected. Metal oxide coating is a natural choice as it is already in the oxidized form and also stable to AO. However, poor flexibility, elaborate sputtering techniques and tendency to crack on thermal cycling are some of the disadvantages. Unlike metal oxide coatings, polymers are soluble in organic solvents and hence can be applied easily. When suitably designed, they exhibit self-healing properties. Nowadays polymers having the self-healing feature have gained the attraction as their property of automatic healing or repairing the surface of the material damaged by the AO erosion. These types of polymers are obtained by incorporating zirconium, phosphorous, silicon and/or titanium. Polyimide (PI) films because of good physical properties, resistance to heat and flexibility are used in the manufacture of flexible electronic gadgets and sensors and also PI-Ag hybrid films are used in flexible conductive material [3-7]. Polysiloxanes, polysilsesquioxanes, p-silahydrocarbons, p-phospazenes, Phosphorus containing polyimides, siloxane-imides, POSS, siloxane-epoxy, decaborane-base polymers, polysilazanes, and carborane siloxanes are used for AO resistant coating materials [8-10].

II. Recent Developments in Atomic Oxygen Resistance Materials

Lian *et al.* [11] reported a monolayered PI composite film named as PI-X film. Poly{amic acids}s {PAA} from {ODA} & {6-FDA} added with various HBPSi were prepared. ODA, HBPSi and DMAc were mixed using a mechanical stirrer at room temperature with under the inert atmosphere (nitrogen) until mixture was fully dissolved.

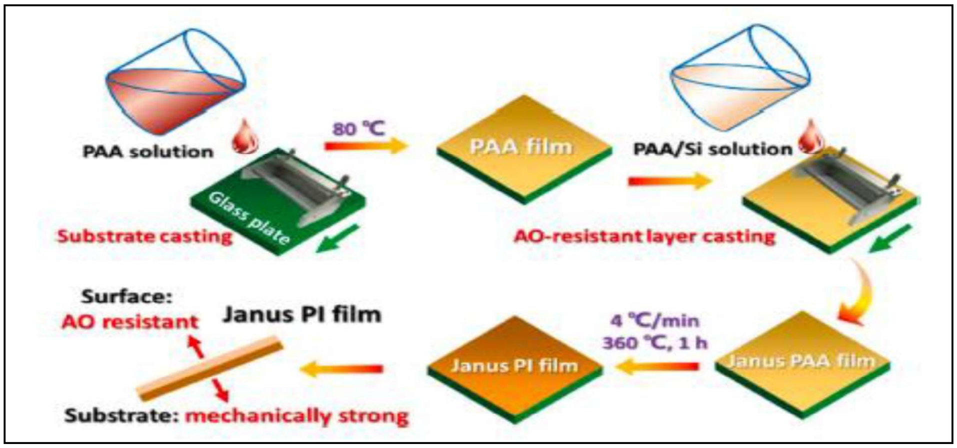

Fig. 1: Preparation Procedure of the Janus Polyimide Film [11]

Later on, adding 6FDA to the solution and stirred at room temperature. Janus PAA film was made by casting the PAA-10 and PAA-20 in oven at 80 °C for 1 hour and then imidizing the janus PAA film kept in an oven for 360 °C for 1 hour, this is known as 'twice-cast strategy' as shown in Fig. 1. The characterized the polyimide (PI) film with the SEM and EDS chart analysis reveals that the interactivity between the substrate layer and the atomic oxygen (AO) layer is smoother without any distribution. In this system 'twice-cast strategy' supplies more strength to the janus structure which doesn't crumble the thermal stability and efficiency of the polyimide backbone. EDS analysis shows that the high concentration of the Si atoms closer to the atomic oxygen (AO) side nourish the interpenetration between the atomic oxygen (AO) layer and the substrate layer during the imidization process. Atomic oxygen property of resistance to polyimide film was examined by the mass loss of polyimide film occurs after by the atomic oxygen (AO) exposure. Janus polyimide (PI) i.e., PI- 40/10 have a mass loss of 8.34% and on other side Kapton H have the mass loss of 7.02%. This minimal decrease in the mass loss % is due to the movement of HBPSi molecules to substrate layer side to atomic oxygen resistance layer side. Considerably, the mass loss % of PI- 40, PI- 40/0 and PI- 40/10 are 033 mg, 058 mg and 039 mg respectively. They also studied the mechanical properties of the polyimide (PI) film. When the HBPSi content increases it reduces the elongation at break, ultimate tensile strength (MPa), tensile modulus (GPa) and toughness (MJ/m3) of the polyimide (PI) film but in monolayered polyimide film, when HBPSi content crosses the 40wt% i.e. PI- 40 its (MPa) holds only ca. 50% that of PI- 0, with elongation at break (%) is very low i.e. 4.7% and holds the 1.57 {MJ/m-3} toughness which shows that the polymer backbone is entirely fragile of PI- 40. While in Janus polyimide (PI) film it manifest more stronger mechanical properties, for example, (MPa) and elongation at break (%) of PI- 40/0 and PI- 40/10 gives the 89 MPa and at 8.0% correspondingly which nearly 1.6 times as compared to PI- 40, also the toughness (MJ/m-3) of PI- 40/10 is 5.22 MJ/m-3 greater than the PI- 40 which is 1.57 MJ/m-3. This gives the confirmation of PI- 40/10 still having the strong polymer backbone with good mechanically robust strength.

Gang *et al.* [12] synthesized HBPSi polyimide films. First, they synthesized the NH_2-HBPSi by adding tetrahydrofuran (THF), ethyl-orhtosilicate (TEOS) and γ-aminopropyl-methyl Diethoxysilane (APMDEOS) in round bottom flask, mechanically stirred, cooled at 0 °C in an ice water bath for 1 hour, and then undergoes rotary evaporation to remove unwanted volatile matter from the product. White powder crude product obtained was kept in vacuum oven for 48 hours at room temperature. The final product is the targeted NH_2-HBPSi. Secondly, (DABA) reacts with DMAc with the proper stirring. After it, BPDA quickly added at room temperature under inert atmosphere (nitrogen). The whole substrate was sheltered by P.A.A. Curing was done at 330 °C. PI films were mixed with the deionized water and dried in a vacuum and finally HBPSi polyimide film obtained as shown in Fig. 2. Characterization of NH_2-HBPSi/ polyimide (PI) film was done by the FTIR in which peak of Si-O-Si vibrations absorbed at 1060 cm-1 show that HBPSi functionalized with amino groups completely. XRD data analysis and FTIR analysis of NH_2-HBPSi and PI film confirms the incorporation of NH_2-HBPSi to the Polyimide (PI) matrix. They also examined the mechanical values of the hybrid film. They studied that the molecular weight of the polyimide has the positive correlation with the mechanical properties of the hybrid film. When NH_2-HBPSi incorporated in the system it effects the Mol.wt of the polyimide. Firstly, system undergoes certain cross-linking reaction when forming the polyamic acid its favorable to increase the molecular weight of polyimide, also the increment in the molecular weight gets obstructed because HBPSi has the good steric-hinderance it exhibits the low reactivity due to the poly-condensation process. Furthermore, NH_2-HBPSi maximizes the molecular chain spacing and minimizes the chain to chain activity. When NH_2-HBPSi at 30wt% it balance the dynamic viscosity of the (PAA) more than the 105 p & the tensile strength of the hybrid-film remains higher than the 225 MPa. It shows that the mechanical values are higher than the Kapton based structure.

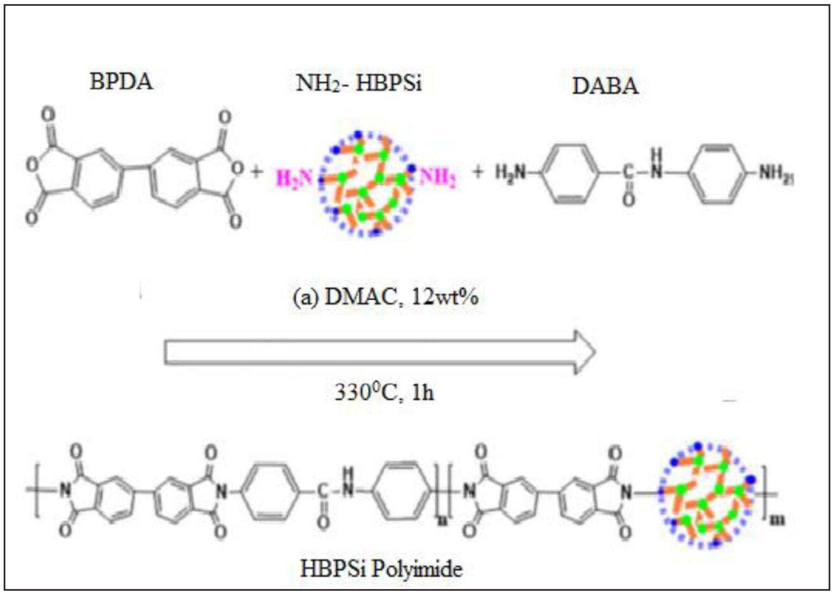

Fig. 2: Process for the Preparation of HBPSi PI Film [12]

Wu *et al.* [13] also prepared the polyimide film with a different monomer i.e. N-{(heptaísobutyl-P.O.S.S)propyl}-3,5-díaminobenzamide (D.A.B.A-P.O.S.S). They synthesized the (DABA-POSS) by hydrogenation of N-{(heptaísobutyl-P.O.S.S)propyl}-3,5-dinítrobenzamide [DNBA-POSS] which undergoes reduction of hydrazine monohydrate with the (Pd/C) catalyst. Ultra-dry DMAc added in three-round bottom flask and mechanically stirred and cooled at -5-0 °C in an ice water bath under continuous nitrogen flow then reacted with the (ODA) and (DABA-POSS). It was continued for 20 hours at room temperature. After some time brownish-yellow thick solution was obtained which was filtered by using the poly-tetrafluoroethylene (PTFE) which gave the PAA20 solution. The PAA20 was casted on a glass substrate. The final product was obtained by curing the substrate at various temperatures in an oven under nitrogen flow.

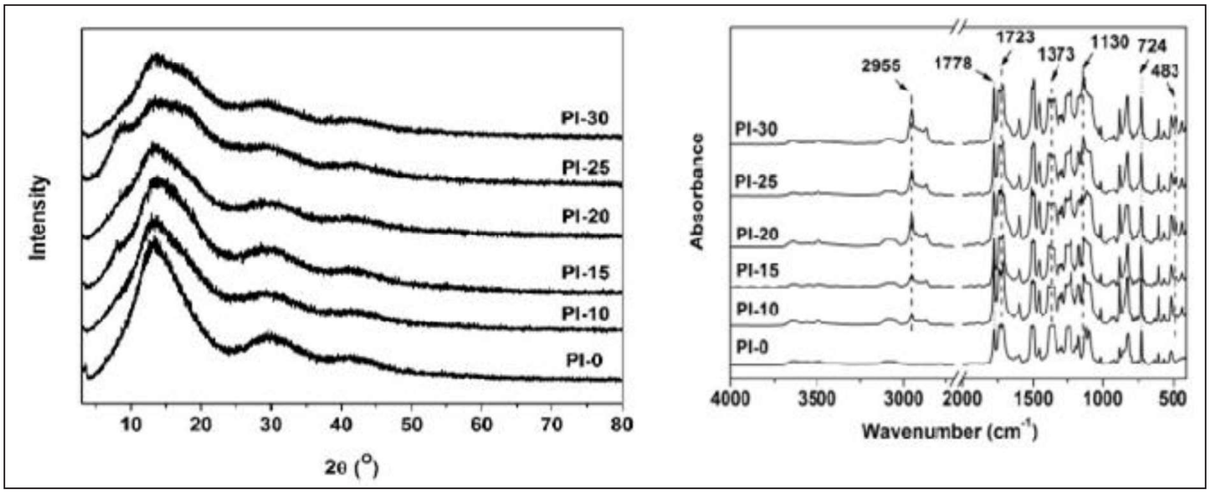

Fig. 3: XRD and FTIR Data of POSS-PI Film [13]

They successfully confirmed the chemical configuration of DABA-POSS diamine by the measurements of FTIR, 1H-NMR and elemental composition. The Fig. 3 gives the information about the FT-IR spectra of the POSS-polyimide (PI) films. The FTIR of the saturated [C H] bond at 2955 cm-1 and Si-o-Si vibrations at 1130 cm-1 which indicated the successful incorporation of P.O.S.S in the Polyimide Film. The P.O.S.S was incorporated successfully in the polyimide (PI) film by copolymerization method instead off adding externally as fillers. Phase-separation was obtained by increasing the amount of D.A.B.A-P.O.S.S. Phase separation is not responsible for the crystallization method of the molecular chain which doesn't causes the transparent visualization of polyimide (PI) film with high P.O.S.S amount. This was confirmed by the X.R.D data.

Li *et al.* [14] synthesized the silver contained polyimide-siloxane film. Considering the accuracy and authentic data solutions were prepared before half a day. Triethylamine and ethylene glycol in respected volume ratios 1:20 reacted with each other to obtain TEA-EG. Opening of ring was done after etching with the KOH solution reacted with the imide group of P.M.D.A-O.D.A. Then PI films used to wash with de-ionized water to makes the ions free surface. Ion exchange was followed for 30 min. After completion, films were again washed by the help of de-ionized water and dried. TEA-EG solution reacted with the PI films and heated for 5 min at 90 °C. De-ionized water was used for washing once the heating completed and then allowed it for drying. Now the ƤAA/Ag composite film introduced as film B was obtained and then imidized ƤI/Ag composite at different temperature conditions as followed the last step is 5 °C/min at 300 °C for 1 hour. The Film was introduced and designated as film C. Similar above process was used for preparing ƤI/silver/ƤI composite film by taking the Ƥ.A.A.S-EG rather than using the TEA-EG. PAAS-EG was synthesized by PI/silver/Ƥ.A.A.S composite film was prepared and named as film Ð and the imidized P.I/silver/P.I composite-film was prepared and named as film E. Now PI/Ag/PI/Ssi-PI composite film was prepared by using the Si-PAAS spinning solution which was synthesized by PI/silver/PI/si/ƤI composite film by 10% and 20% Si-Ƥ.A.A.S solution was named as film F and film G. The characterized the PI/silver/PI composite film and the Polyimide/silver/PAAS composite film shows the peaks at 1670 cm-1 due to amide group and at 1740 cm-1 due to the stretching-vibrations of the C=O bond of the R-COOH. But the deep peak was absorbed at 1080 cm-1 which confirmed that Si-O-Si present in the system. They also done the conductivity test in which they found that only the surface of the film was conductive as it has the low resistance and dense silver (Ag) layer. Other two composites film shows very high resistance and has the insulation property. This indicates that the different insulating surfaces of the PI/Ag/PI films were prepared to obtain the resistance properties of the films i.e. surface of the Polyimide/silver film is conductive and two types of the surfaces of the PI/silver/PI films are insulated.

Xu *et al.* [15] studied about polysiloxane flexible shielding for LEO spacecraft with ultra efficient AO and self healing behavior. Hexamethyldisiloxane (HMDSiO) used for preparation of a plasma polymerizes easily bendable film. This film used for the surface coating on Kapton. This process was done by three steps, they are: (i) excitation of argon used for the activation and etching of the Kapton. (ii) Polymerisation at constant flow rate of HMDSiO vapor, oxygen, and Argon. (iii) Nitrogen passed to the film and maintained atmospheric pressure. Difference in coefficient of thermal expansion between Kapton film and coatings causes development of compressive stress. Polysiloxane coatings improve the thermal and AO properties. Reliability and flexibility was investigated by using the thermal cycling and bending test. These tests are conducted in various parameters such as different temperature and thermal cycles. Bending test was conducted for several times. Self healing behavior of the polysiloxane obtained from the structural and compositional evolution during the AO irradiation procedure depends on the high uniformity and strong interfacial behavior. SEM images gave the information about the surface properties of the coating. Self healing changes the surface properties but it does not cause the cracks and defects. It also changes the composition of the coating from pure poly-HMDSiO to SiO_2/Poly-HMDSiO hybrid material. XPS tells about the characterization of AO irradiation. Peaks in the XPS related to the $SiO_2$and poly-HMDSiO. XPS peaks show the surface morphology changes from pure HMDSiO to SiO_2-HMDSiO hybrid. Polysilane coatings shows the ductile brittle transformation and micro scale needle like cracks fully covered the surface of the P-HMDSiO coatings caused by the AO irradiation. It also causes the internal stress. SEM image and XPS images shown below.

III. CHARACTERIZATION TECHNIQUES FOR AO RESISTANCE MATERIALS

Characterizing atomic oxygen (AO) resistance in materials is essential to ensure spacecraft durability in low Earth orbit. Key characterization techniques include as shown in Fig. 4.

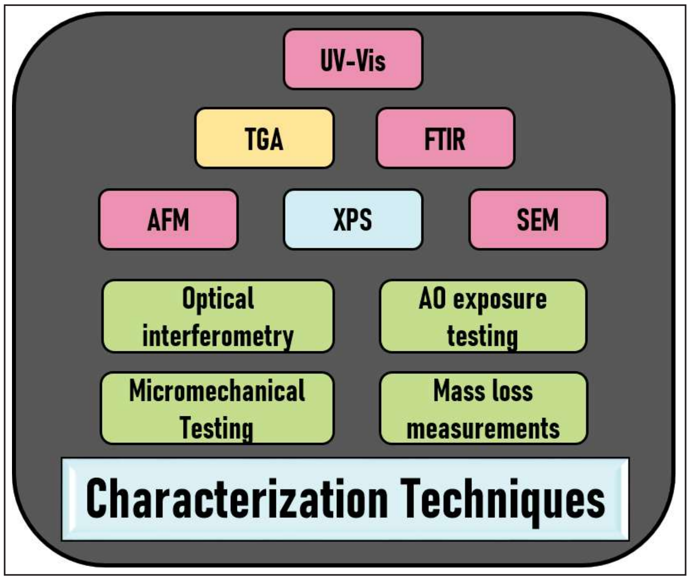

Fig. 4: Characterization Techniques for AO Resistant Materials

- *AO Exposure Testing:* Simulated AO environments are created in ground-based facilities, like RF plasma asher systems or atomic oxygen beam sources, to mimic LEO conditions. These setups allow direct assessment of material erosion rates and degradation under controlled AO exposure [16].
- *Mass Loss Measurements:* By measuring the mass loss of materials after AO exposure, researchers can quantify the erosion rate. This is a direct indicator of AO resistance, particularly for polymers and other erosion-prone materials [17].
- *Surface Morphology Analysis*
  - *Scanning Electron Microscopy (SEM):* SEM provides detailed imaging of surface changes and erosion patterns post-AO exposure [18].
  - *Atomic Force Microscopy (AFM):* AFM offers high-resolution surface topography data to reveal surface roughness and morphological changes on the nanoscale.
- *Spectroscopic Techniques*
  - *X-Ray Photoelectron Spectroscopy (XPS):* XPS analyzes elemental composition and chemical bonding changes on material surfaces after AO exposure, particularly useful for tracking oxidation.
  - *Fourier Transform Infrared Spectroscopy (FTIR):* FTIR detects specific chemical groups altered by AO, helping to assess molecular-level changes in polymeric materials [19].
- *Optical Interferometry:* This non-contact technique measures surface topography changes, allowing precise tracking of material thickness loss due to AO erosion.
- *Micromechanical Testing:* Nano indentation and scratch tests provide information on changes in hardness and adhesion, which can indicate material degradation and reduced mechanical integrity after AO exposure [20].
- *Thermogravimetric Analysis (TGA):* TGA evaluates thermal stability changes due to AO exposure by monitoring weight loss at varying temperatures, offering insight into material robustness.
- *Ultraviolet-Visible (UV-Vis) Spectroscopy:* For polymer-based AO-resistant materials, UV-Vis can reveal changes in optical properties, indicating surface degradation or oxidation.

Together, these techniques provide a comprehensive understanding of material resilience to AO, aiding the development of advanced coatings and composites for space applications.

IV. Polymers Used in AO Materials

- *Fluorinated Polymers*

Fluorinated polymers are often resistant to atomic oxygen attack because the C-F bond is oxidised endothermically. Teflon degrades ten times more slowly than polyethylene. The Long Duration Exposure Facility (LDEF), which was opened in April 1984, allowed researchers to investigate the effect of atomic oxygen on FEP Teflon (fluorinated ethylene-propylene polymer) [21].

Poly[bis(trifluoroethoxy)phosphazene] films were found to be resistant to atomic oxygen exposure due to backbone rearrangements, crosslinking, and the creation of phosphorus-oxygen and nitrogen-oxygen bonds [22].

- *Carborane-Siloxane Polymers*

Though silicones generate a protective SiO_2 layer when reacting with atomic oxygen, they tend to shatter or craze due to volume shrinkage, as previously stated. Adding carborane units to the siloxane backbone can address this issue. A carborane moiety has 10 boron atoms and will absorb 15 oxygen atoms upon oxidation. Carborane-siloxane polymers can gain around 50% weight when exposed to atomic oxygen, compensating for volume shrinkage caused by increased density (from ~1 to ~1.92 g cm 3 for $B_{10}O_{15}.(SiO_2)_3$). Many studies reveal that incorporating carborane-siloxane polymers increases the layer compressive stress [23, 24].

- *Decaborane Based Polymers*

Decaborane ($B_{10}H_{14}$) interacts with Lewis bases such amines, phosphines, sulphides, and nitriles to generate $B_{10}H_{12}.2L$ adducts [25]. When both Lewis base sites are present in the same molecule, a linear polymer can form.

In the early 1960s, researchers reported the synthesis of decaborane-based linear polymers from Lewis bases, including amines, amides, nitriles, and phosphines. Although these polymers were supposed to be useful for high-temperature stability and high-energy fuels, their use as boron-containing preceramic polymers was not recognised. Recent studies have explored the use of decaborane-based polymers as precursors for boron carbide and boron nitride [26-28].

V. METHODS OF SATELLITE-BASED ATOMIC OXYGEN SENSING

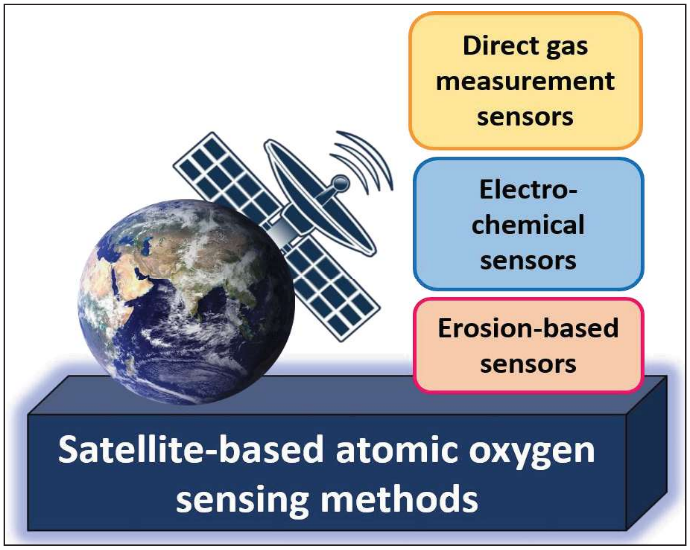

Fig. 5: Three Methods of Satellite-Based AO Sensing

Spacecraft orbiting Earth face significant environmental dangers. Spacecraft engineering has focused on preventing risks such ultra-high vacuum, ionising radiation, and extreme temperature cycles. One threat, however, has become increasingly relevant over the past few years [29].

Atomic oxygen (AO) is the most prevalent atmospheric gas species found in the residual atmosphere between 170 and 700 kilometers altitude. At lower altitudes, the atmosphere blocks UV sun radiation, causing diatomic oxygen to dissociate [30]. As the satellite industry focusses on low-altitude satellites, it is crucial to improve our understanding of the AO environment and its impact on satellite performance. There are three types of AO sensors: those that directly monitor gas species, those that measure electrochemical changes, alongside those that record the rate of erosion of a sacrificial substance as represented in Fig. 5 [31].

- *Direct Gas Measure Sensing Method*
    - *Chemiluminescence:* The first approach for detecting atomic oxygen flux was through the 'Shuttle Glow' phenomenon, which was discovered during space shuttle launch and descent. The recombination of atomic oxygen and NO molecules on the shuttle's surface, resulting in NO_2, cause shuttle light [32]. However, no single reaction mechanism accounts for all wavelengths of shuttle glow emission. Chemiluminescence remains a niche attraction due to its durability and simplicity. The NO tank, nozzles, and spectrometer system are extremely resistant to contamination and damage. During reentry, chemiluminescence measurements were used to monitor atomic oxygen flux, which would otherwise destroy other sensor and detection systems.
    - *Mass-Spectrometry:* Despite being introduced in the beginning stages of AO sensing, mass spectrometry (MS) equipment is still employed in missions that require accurate results, gas composition, or velocity data [33]. MS technique was previously utilised to measure gas phase species concentrations at low pressures, making it a natural fit for space applications. Mass spectrometry remains significant for current AO measurement due to its ability to eliminate variables that can negatively impact accuracy in other sensors. UV radiation, other gas species, and thermal cycling have no impact on AO MS results.
- *Electro-Chemical Sensing Method*
    - *Actinometry:* Actinometers detect atomic oxygen by detecting the change in electrical resistance when a closed circuit is partially exposed to the atmosphere. When subjected to an AO flow, electrically conductive materials like silver or osmium undergo erosion and conversion into non-conductive oxides. Henderson and Schiff developed a unique AO flux sensor [34]. As demand for lower-altitude satellites grew, flux sensors became lighter and less sophisticated than shuttle glow or mass spectrometry.
    - *FIPEX Sensors:* FIPEX (Flux-Phi-Probe Experiments) sensors are new atomic oxygen sensors that use yttria-doped zirconia (YSZ). Although YSZ-based sensors have been used on sounding rockets to measure O_2 concentrations with altitude for years, they have just recently been utilised to detect AO.FIPEX sensors detect the rate of oxygen adsorption on exposed solid oxide electrodes like YSZ. Adsorption of AO atoms on an electrode results in the formation of oxygen ions [35].
- *Erosion-Based Sensing Method*
    - *Optical Degradation:* Optical degradation sensors are ideal for nanosatellites due to their lightweight design and simplicity. Optical degradation methods are ideal for missions with limited mass and budget, as sensors typically consist of a photovoltaic cell, sacrificial material, and an electrical connection. Optical degradation sensors have been shown to be as light as 8 g [36].
    - *Witness Samples:* However, there are substantial downsides. Witness samples are small patches of material put on a satellite's outer surface and subjected to the VLEO environment for several months or years.

A sample's mass and volume are evaluated prior to and following flight to assess environmental deterioration over time. This analysis estimates the total AO fluence seen by the specimen over its lifetime based on the erosion rate per impinging oxygen atom. To assess witness samples in a lab setting, the spacecraft must be recoverable. AO flux data are averaged over the flight. Ex situ measurement prevents missions from receiving erosion data during operation and spacecraft from reacting to witness samples [37].

- *Quartz Crystal Microbalance:* QCMs are a derivative of the witness sample measurement approach. The witness sample is mounted on an oscillating crystal, and its mass is determined over time using the crystal's resonance frequency [38].

VI. Conclusion

Developing atomic oxygen (AO)-resistant materials is crucial for the longevity and performance of spacecraft operating in low Earth orbit (LEO). Exposure to AO poses a significant threat, particularly to polymers and other organic materials, causing surface erosion, mass loss, and functional degradation. Advances in AO-resistant materials, such as ceramic and metal coatings, fluorine-based polymers, and hybrid composites, offer promising solutions for protecting spacecraft surfaces. Protective coatings like silicon oxide and aluminum oxide have proven effective in reducing AO-induced erosion, while nanostructured and fluorine-rich materials show potential due to their enhanced stability and lightweight nature. Furthermore, advanced simulation techniques and ground-based AO exposure testing allow for accurate characterization of material performance, guiding the optimization of AO-resistant technologies. Spectroscopic and morphological analyses provide detailed insights into surface changes, helping researchers refine materials to withstand AO exposure more effectively. As space, missions expand in duration and complexity, developing materials that resist AO damage becomes increasingly important for mission safety, cost-efficiency, and reliability. Continued research into AO-resistant materials will support the advancement of long-lasting spacecraft components, contributing to safer and more sustainable space exploration.

Acknowledgment

The author would like to thank Sharda University for the publication.

References

[1] S. Packirismay, D. Schwam, and M. H. Litt, "Atomic oxygen resistant coatings for low Earth orbit space structures," *J. Mater. Sci.*, vol. 30, no. 2, pp. 308-320, 1995

[2] M. R. Reddy, "Effect of low Earth orbit atomic oxygen on spacecraft materials," *J. Mater. Sci.*, vol. 30, no. 2, pp. 281-307, 1995.

[3] S. J. Choi, S. J. Kim, J. S. Jang, J. H. Lee, and I. D. Kim, "Silver nanowire embedded colorless polyimide heater for wearable chemical sensors: Improved reversible reaction kinetics of optically reduced graphene oxide," *Small*, vol. 12, no. 42, pp. 5826-5835, 2016.

[4] W. Song, J. Zhu, B. Gan, S. Zhao, H. Wang, C. Li, and J. Wang, "Flexible, stretchable, and transparent planar microsupercapacitors based on 3D porous laser-induced graphene," *Small*, vol. 14, no. 1, p. 1702249, 2017.

[5] D. Li, W. Y. Lai, Y. Z. Zhang, and W. Huang, "Printable transparent conductive films for flexible electronics," *Adv. Mater.,* vol. 30, no. 10, p. 1704738, 2018.

[6] A. Goto, K. Umeda, K. Yukumatsu, and Y. Kimoto, "Property changes in materials due to atomic oxygen in the low Earth orbit," *CEAS Space J.*, vol. 13, no. 3, pp. 415-432, 2021.

[7] D. Devapal, S. Packirisamy, R. M. Korulla, and K. N. Ninan, "Atomic oxygen resistant coating from poly (tetramethyldisilylene-co-styrene)," *J. Appl. Polym. Sci.*, vol. 94, no. 6, pp. 2368-2375, 2004.

[8] L. Ji, H. Li, F. Zhao, W. Quan, J. Chen, and H. Zhou, Atomic oxygen resistant behaviors of Mo/diamond-like carbon nanocomposite lubricating films," *Appl. Surf. Sci.,* vol. 255, no. 7, pp. 4180-4184, 2009.

[9] K. Xie, W. Wang, Y. Li, M. Xu, Z. Han, Y. Zhang, and W. Gao, "Study on structure-performance relationship of RGO enhanced polypropylene composites with improved atomic oxygen resistance," *Compos. B Eng.,* vol. 239, p. 109970, 2022.

[10] R. H. Hansen, J. V. Pascale, T. De Benedictis, and P. M. Rentzepis, "Effect of atomic oxygen on polymers," *J. Polym. Sci., Part A: Gen. Pap.,* vol. 3, no. 6, pp. 2205-2214, 1965.

[11] R. Lian, X. Lei, S. Xue, Y. Chen, and Q. Zhang, "Janus polyimide films with outstanding AO resistance, good optical transparency and high mechanical strength," *Appl. Surf. Sci.,* vol. 535, no. 1, p. 147654, 2021.

[12] L. V. Gang, S. Xie, D. Mao, G. Ren, S. Wu, and W. Yang, *High Perform. Polym.,* vol. 33, no. 8, p. 924, 2020.

[13] H. Wu, Y. Zhang, Y. D. Guo, H. R. Qi, Y. C. An, Y. J. Jia, Y. Y. Tan, J. G. Liu, and B. H. Wu, "Preparation and properties of intrinsically atomic-oxygen resistant polyimide films containing polyhedral oligomeric

silsesquioxane (POSS) in the side chains," *Polym.,* vol. 12, no. 12, p. 2865, 2020.

[14] L. Li, C. Liu, C. Qu, S. Zheng, D. Wang, J. Chang, D. Zhao, Y. Tang, X. Fan, Z. Liu, W. Xiao, and H. Yang, "In-Situ self-encapsulated flexible multi-layered poly (imide siloxane) copolymer film with resistance to atomic oxygen," *Mater. Today Commun.*, vol. 23, p. 100959, 2020.

[15] M. Xu, Y. Zhao, X. Zhang, Z. Li, L. Zhao, Z. Wang, and W. Gao, "Highly homogeneous polysiloxane flexible coating for low earth orbital spacecraft with ultraefficient atomic oxygen resistance and self-healing behavior," *ACS Appl. Polym. Mater.,* vol. 1, no. 12, p. 3253-3260, 2019.

[16] M. Zhao, F. Si, C. Liu, Y. Lu, Y. Wang, S. Wang, Y. Zeng, Y. Jiang, H. Zhou, and W. Liu, 'Effect of AO/UV/RD exposure on spaceborne diffusers: A comparative experiment," *Appl. Opt.,* vol. 54, no. 31, pp. 9157-9166, 2015.

[17] G. W. Sjolander, "Atomic oxygen-metal surface studies as applied to mass spectrometer measurements of upper planetary atmospheres," *J. Geophys. Res.,* vol. 81, no. 22, pp. 3767-3770, 1976.

[18] A. Delfini, F. Santoni, F. Bisegna, F. Piergentili, R. Pastore, A. Vricella, M. Albano, G. Familiari, E. Battaglione, R. Matassa, and M. Marchetti, "Evaluation of atomic oxygen effects on nano-coated carbon-carbon structures for re-entry applications," *Acta Astronaut.,* vol. 161, pp. 276-282, 2019.

[19] R. Larciprete, P. Lacovig, S. Gardonio, A. Baraldi, S. Lizzit, "Atomic oxygen on graphite: Chemical characterization and thermal reduction," *J. Phys. Chem. C.*, vol. 116, no. 18, pp. 9900-9908, 2012.

[20] H. M. Gardner, P. Gopon, C. M. Magazzeni, A. Radecka, K. Fox, D. Rugg, J. Wade, D. E. J. Armstrong, M. P. Moody, and P. A. J. Bagot, "Quantifying the effect of oxygen on micro-mechanical properties of a near-alpha titanium alloy," *J. Mater. Res.,* vol. 36, pp. 2529-2544, 2021.

[21] B. A. Banks, L. Gebauer, and C. M. Hill, 1st LDEF Post-Retrieval Symposium, 1991.

[22] L. L. Fewell, "Atomic-oxygen induced structural changes in polyphosphazene films and coatings," *J. Appl. Polym. Sci.,* vol. 41, no. 1-2, pp. 391-406, 1990.

[23] D. Schwam, J. Kulig, and M. H. Litt, "X-ray photoelectron spectroscopic depth profiling of an atomic oxygen resistant poly (carborane-siloxane) coating," *Chem. Mater.*, vol. 3, no. 4, pp. 616-620, 1991.

[24] D. Nir, "Stress relief forms of diamond-like carbon thin films under internal compressive stress," *Thin Solid Films,* vol. 112, no. 1, pp. 41-50, 1984.

[25] L. Gmelin, *Gmelin Handbook of Inorganic Chemistry*, 8th ed. Germany: Springer, 1984, pp. 151-165.

[26] H. J. Schroeder, J. R. Reiner, and T. L. Heying, *lnorg. Chem.,* vol. 1, p. 618, 1962.

[27] D. Seyferth, W. S. Rees Jr, A. Lightfoot, and J. S. Haggerty, "Preparation of boron-containing ceramic materials by pyrolysis of the decaborane(14)-derived [B10H12.cntdot.Ph2POPPh2]x polymer," *Chem, Mater.,* vol. 1, pp. 45-52, 1989.

[28] D. Seyferth, and W. S. Rees Jr, "Preparation, characterization, and pyrolysis of [-B10H12. cntdot. diamine]-n polymers: A new route to boron nitride," *Chem. Mater.,* vol. 3, pp. 1106-1116, 1991.

[29] J. Weerasinghe, K. Prasad, J. Mathew, E. Trifoni, O. Baranov, I. Levchenko, and K. Bazaka, "Carbon nanocomposites in aerospace technology: A way to protect low-orbit satellites," *Nanomater.,* vol. 13, no. 11, p. 1763, 2023.

[30] L. Heroux, and H. E. Hinteregger, "Aeronomical reference spectrum for solar UV below 2000 Å," *J. Geophys. Res. Space Phys.,* vol. 83, no. A11, pp. 5305-5308, 1978.

[31] B. E. Holmes, V. T. Oiko, and P. C. Roberts, "A review of satellite-based atomic oxygen sensing methods," *Prog. Aerosp. Sci.,* vol. 137, p. 100886, 2023.

[32] R. A. Viereck, E. Murad, B. D. Green, P. Joshi, C. P. Pike, R. Hieb, and G. Harbaugh, "Origin of the shuttle glow," *Nature*, vol. 354, no. 6348, pp. 48-50, 1991.

[33] M. Kaufmann, Y. Zhu, M. Ern, and M. Riese, "Global distribution of atomic oxygen in the mesopause region as derived from SCIAMACHY O(^{1}S) green line measurements," *Geophys. Res. Lett.,* vol. 41, pp. 6274-6280, 2014.

[34] J. J. Osborne, I. L. Harris, G. T. Roberts, and A. R. Chambers, "Satellite and rocket-borne atomic oxygen sensor techniques," *Rev. Sci. Instrum.,* vol. 72, no. 11, pp. 4025-4041, 2001.

[35] Y. Cheng, X. Chen, and T. Sheng, "In situ measurement of atomic oxygen flux using a silver film sensor onboard "TianTuo 1" nanosatellite," *Adv. Space Res.,* vol. 57, no. 1, pp. 281-288, 2016.

[36] R. Verker, A. Bolker, Y. Carmiel, I. Gouzman, E. Grossman, T. K. Minton, and S. Remaury, "Ground testing of an on-orbit atomic oxygen flux and ionizing radiation dose sensor based on material degradation by the space environment," *Acta Astronaut.,* vol. 173, pp. 333-343, 2020.

[37] C. T. G. Smith, M. Delkowki, J. V. Anguita, D. C. Cox, C. Haas, and S. R. P. Silva, "Complete atomic oxygen and UV protection for polymer and composite materials in a low Earth orbit," *ACS Appl. Mater. Interfaces.,* vol. 13, no. 5, pp. 6670-6677, 2021.

[38] K. Nishiyama, and H. Kuninaka, *Trans. Jpn. Soc. Aeronaut. Space Sci.,* vol. 12, p. 19, 2014.